International Journal of Technical Innovation in Modern Engineering & Science (IJTIMES)
Impact Factor: 5.22 (SJIF-2017), e-ISSN: 2455-2585
Volume 4, Issue 6, June-2018

ANFIS BASED Single-Phase Dual-Stage Isolated Multilevel Inverter Applied to Solar Energy Processing

P.Bhaskara Prasad[1], R.Madan Mohan[2], T.Nithin Sagar[3]
Department of EEE, AITS Rajampet,bhaskara.papugari@gmail.com
Department of EEE, AITSRajampet,madhanmohanmadhu@gmail.com
Department of EEE, AITS Rajampet,nithinsagar42@gmail.com

Abstract— This paper presents single-phase Dual stage multilevel inverter applied to solar energy processing .The processing of PV panel was done by using Dual-stage inverter through galvanic isolation .The circuit consist of a DC-DC Resonant converter ,Transformer .The Transformer secondary is connected to Graetz circuits having connection with NPC .The objective of DC-DC Resonant converter is providing voltage to the inverter .The DC-AC conversion stage consist of Mono-Phase NPC which plays important role in grid current control and capacitive bus control . Inverter control loops are obtained by using two different modelling methods. By using the operation stages internal transfer function is obtained and using reverse energy flow external transfer function is assessed. The simulation results presented in this project are carried out in MATLAB/SIMULINK with following specifications:2KW output power: 400V input voltage,127 V_{rms} Ac output voltage .

Keywords— photovoltaic multi-level inverter; dual-stage inverter; inverter applied in alternative sources of energy; electronic processing of solar energy.

I.INTRODUCTION

Currently in the energy scenario, both the availability and the quality of energy are determining factors for the development of a country. Brazil has developed a predominantly hydroelectric energy generation matrix, dependant on hydrological cycles. However, with the increase in population and industrial production, the country has had problems of water shortage, leading to energy crises like the one that occurred in 2001 [1], [2].The growing concern with environmental issues has increased over the years, as well as the diversification of the country's energy matrix: solar, wind, biomass, among others. In global parameters, there was a 17% increase in renewable energy investment in 2014 compared to 2013. In developing countries, there was a 36% increase over the previous year. According to a report from the United Nations Environment Program (UNEP), China was the country that invested the most in this area with 83.3 billion dollars. Brazil, in 2014, invested 7.6 billion dollars, followed by India with 7.4 billion and South Africa with 5.5 billion. These last three countries are among the ten top investors in renewable energy in the world. With these data, it is possible to perceive the importance and the tendency to explore new sources of alternative energy [3].This paper has focused on the generation of electricity from solar photovoltaic modules. When the solar modules are connected to the AC grid, there is an increase in the supply of energy near the load centers, but in order to inject the energy converted by the modules it is necessary to use static power converters [4]. There are several converter topologies, with one or two stages, and control techniques used for power processing in PV systems [4]–[9].In two-stage topologies, it was observed that there is no use of a multilevel inverter NPC (Neutral Point Clamped) in their compositions. Thus, this paper presents the implementation of a two-stage inverter, featuring a three-level NPC inverter in its structure. The main advantages of the proposed structure are: the natural clamping of the NPC; voltage division on actives witches; dv / dt reduction; reduced volume and filter inductor weight due to the three voltage levels in the load, thus contributing to a faster dynamic, besides reducing the response time of the structure; and the lack of need for control on the DC side of the structure [10], [11]. The main disadvantages of the structure are: more components when compared to single stage structures; the necessity to isolate the control circuit in order to actuate the active switches in different references; and the use of high frequency transformer with two secondary. The proposed topology is shown in Section II.

In Section III, the use of the DC-DC converter is discussed. In Section IV, the operating steps of the inverter are presented, its operation is described and its main equations are defined. Section V presents the obtaining of the functions of transfer of the inverter and its modeling. In Section VI, the obtained simulation results are shown. Finally, Section VII presents the conclusion. The first stage is composed of a DC-DC series resonant converter and a transformer, both three-phase and operating at high frequency, thus reducing the size and weight of the transformer. Because of its topological peculiarity, the DC-DC converter can operate with soft switching, both ZCS (zero current switching) and ZVS (zero voltage switching) reducing system losses [13]. In this way, it was used as ZCS, equaling the switching frequency with the resonant frequency. The secondary windings of the transformer are connected to two Graetz bridges, which are connected to the capacitive bus NPC inverter. The second stage consists of the NPC inverter, responsible for the injection of the current in the electric grid, besides being controlled by the internal and external transfer functions. Fig. 1 shows the proposed inverter. The NPC inverter requires a separate control to keep the voltage on its capacitive bus equally divided [14]. However, one of the differentials of the proposed structure is the use of a DC-DC converter, which has the objective of generating a capacitive bus with equally divided voltages for the NPC, not having to develop control for it. The DC-DC converter is simplified in Fig. 2, where the line inductances represent the inductances of the transformer and *Rloss* the losses distributed by the circuit. Based on the DCDC converter series resonant [13], this converter has interesting features like: operation with soft switching of the ZCS type (switching frequency equal to resonance), high switching frequency, high efficiency The DC-DC converter operates with equivalent capacitive and inductive reactance. Thus, it is possible to verify that there is a simultaneous switching of the diodes from Graetz bridges in relation to the DC-DC converter transistors. Then, the voltages at points A, B and C of the converter are in phase with the voltages at points a, b and c, respectively, as shown in Fig. 2. Therefore, the resulting voltage on the RLC circuit is the difference between these voltages. Following the methodology presented .The first step is the moment when the active switches S1 Fig. 3. NPC inverter operation steps. And S2 are turned on and S3 and S4 are turned off. In this step there is transfer of energy from the capacitor C1 to the load vCA, leading to a positive voltage in the latter. In the second step, S1 and S4 are turned off and S2 and S3 are turned on. Due to the positive half-cycle of the modulating sine wave there is current flow only through the clipping diode Ds1, causing a freewheeling step of the inverter. Therefore, there is no transfer of energy from the capacitor C1 to the load, leaving it with zero voltage level.

II. PROPOSED TWO-STAGE INVERTER

The proposed topology is a change on the circuit utilized by [12], and the favorable advantages are because of the utilization of a multilevel inverter and no need to make an appropriate control to balance the voltage on the capacitive bus NPC due to the DC-DC converter. The primary stage is made out of a DC-DC Resonant converter and a transformer, both three-phase and Operating at high frequency, thus reducing size and weight the size and weight of the transformer. Due to its topological characteristic, the DC-DC converter can work with soft switching's, both ZCS (zero current exchanging) and ZVS (zero voltage exchanging) decreasing system losses[13].Thus it is used as ZCS equalizing resonant frequency with switching frequency. The secondary windings of the transformer are connected with two Graetz bridges, which are connected with the capacitive bus NPC inverter. The second stage comprises of the NPC inverter, responsible for current injection in to the grid, besides being controlled by the internal and external transfer function. . Fig. 1 shows the proposed inverter

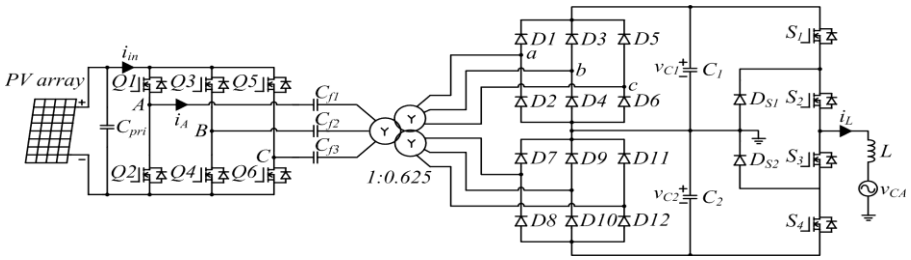

Fig. 1 Structure of the proposed two-stage inverter

III. DC-DC CONVERTER

The NPC inverter needs a separate control to keep the voltage on its capacitive bus equally divided [14]. The proposed structure is one of differential use of a DC-DC converter, which is responsible of generating a capacitive bus with equally divided voltages for the NPCFig.2 shows the simplified DC-DC converter, where the line inductances are the inductances of the transformer and R_{loss} *are the* losses by the circuit. Depending on the DC-DC converter series resonant [13], this converter has interesting features like: operation with soft switching of the ZCS type (switching frequency equal to resonance), high switching frequency, high efficiency [12], [13], [15].

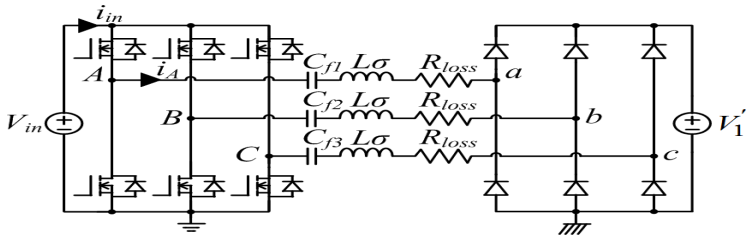

Fig. 2 Transformer less DC-DC converter

A. Output voltage ratio with the input

The DC-DC converter works with equal capacitive and inductive reactance. Thus, it is possible to verify that there is a simultaneous switching of the diodes from Graetz bridges is in connection with the DC-DC converter transistors. Now,At this points A, B and C of the converter are in phase with the voltages at points a, b and c, respectively, as shown in Fig. 2. Therefore, the voltage obtained on the RLC circuit is the difference between these voltages. Following the methodology presented by [13], it is possible to obtain (1).

$$i_A = \frac{2}{\pi}\frac{1}{R_{loss}}\left(V_{in} - V'_{loss}\right)\sin(wt) \quad (1)$$

Where R_{loss} represents the parasitic resistances distributed by the circuit; V_{in} is the input voltage of the converter; V'_1 is the reflected output voltage; i_A is the line current of the converter. The phase current (i_A) is equal to the input current (i_{in}) in the range of 60 ° to 120 °. The average value of this current can be obtained by (2).

$$I_{INMED} = \frac{6}{\pi^2}\frac{1}{R_{LOSS}}(V_{in} - V'_1) \quad (2)$$

Therefore the input powers (3) and output (4) of the DCDC converter are calculated [12].

$$P_{IN} = V_{in} I_{nmed} \quad (3)$$

$$P_{1=} V'_1 I_{med} \quad (4)$$

From (3) and (4) the efficiency of the DC-DC converter can be obtained in (5).

$$n = \frac{V'_{out}}{V_{in}} \quad (5)$$

The efficiency DC-DC converter is high about 97% [13], the efficiency can be approximated to a unit value. This shows that in (5) there is a direct relation between the output voltage and the input.

IV. OPERATION STEPS AND PRIMORDIAL INVERTER EQUATIONS

The modulation strategy used for active switches was by level shift, specifically the IPD (In Phase Disposition). In this modulation, the triangular carriers have the similar frequency and amplitude, but they are displayed vertically in such a way that the bands occupied by each one are distinct and in phase [11].

A. NPC operation steps

In this paper, the ideal NPC inverter was considered. Thus, by the modulation used, the inverter has four operating stages, all shown in Fig. 3.

In first step at this instant the active switches S_1 and S_2 are turned on and S3 and S4 are turned off. In this step there is transfer of energy from the capacitor C_1 to the load V_{CA}, leading to a positive voltage in the latter.

In the second step, at this moment S_1 and S_4 are turned off and S_2 and S_3 are turned on. Due to the positive half-cycle there is current flow only through the clipping diode D_{s1}, causing a freewheeling step of the inverter. Due to this no transfer of energy from the capacitor C_1 to the load, leaving it with zero voltage level.

In the third step first and second steps are repeated until the negative half-cycle of the modulating sine wave begins. This cause S_1 and S_2 are turned off, but S3 and S4 are turned on. Thus there is energy transfer from C2 to the V_{CA} load, causing a negative voltage to appear in the latter.

Finally, in same way as in the second step, S_1 and S_4 are turned off and S_2 and S_3 are turned on in fourth step. Due to the negative half-cycle of the modulating sine wave there is current flow only through the clipping diode D_{s2}, causing a free-wheeling step of the inverter. The third and fourth steps are repeated until the positive half-cycle of the modulating sine wave starts, returns to the first step of operation.

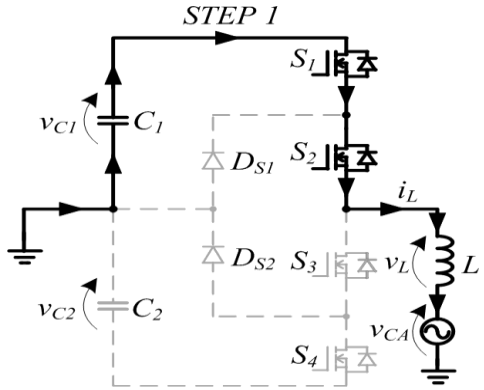

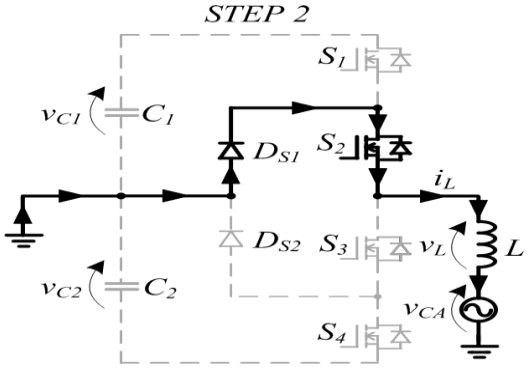

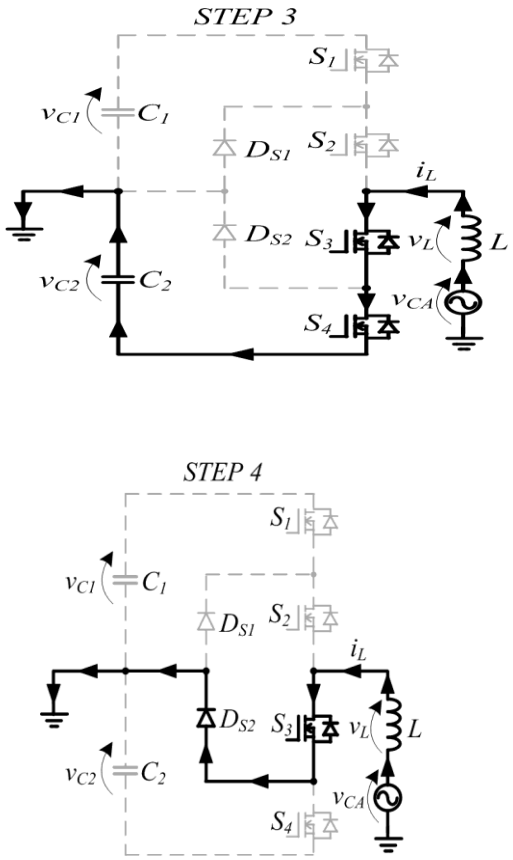

Fig. 3 NPC inverter operation steps

B. Main inverter calculations

In order to obtain the value of the main components of the inverter, its first and second stages of operation were used. Fig. 4 was used to develop the equations of this subsection.

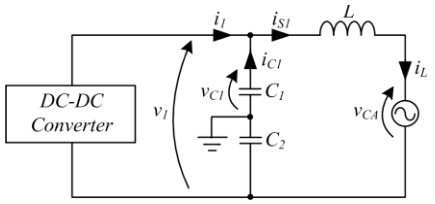

Fig.4NPC equivalent circuit for step of opeartion

1) ***Static gain:*** A mesh analysis was carried out in the two steps of operation, isolating the current derivative of the inductor in both, and making a weighted average of them, arriving at (6). With V1 being the sum of the voltages of VC1 and VC2.

$$\frac{di_l}{dt} = \frac{v_1}{2L}D - \frac{V_{CA}}{L} \qquad (6)$$

Where: V_1 is the voltage across the NPC bus; V_{CA} is the grid voltage; D is the duty cycle; L is the inductance of the output filter; diL / dt is the instantaneous derivative of current in the inductor. We known that the current derivative of the steady state inverter is zero.

Thus, (6) gives to (7), representing the output characteristic of the inverter as a function of its duty cycle D. It is also observed that the voltage V1 must be at least twice higher than the V_{CA} peak.

$$\frac{V_{CA}}{V_1} = \frac{D}{2} \tag{7}$$

*2) **Calculation of the output inductor**:* The output inductor injects current in to the grid to which gives the sine wave [16]. From (7) and considering that D has a sinusoidal envelope, there is (8).

$$D(\omega_{grid}\, t) = \frac{2}{V_1} V_{CAP}\ \sin(\omega_{grid}\, t) \tag{8}$$

Where: V_{CAp} is the peak voltage of the power grid; *grid* ω is the angular frequency of the grid. Applying a mesh analysis to the first step of the inverter,(9) is obtained.

$$\Delta i_L = \frac{V_1 D}{2 f_s L} - \frac{V_{CA} D}{f_s L} \tag{9}$$

Where: fs is the switching frequency; Δi_L is the ripple in the inductor. Putting (8) into (9) gives (10).

$$\Delta i_L = \frac{V_{CAP} \sin(\omega_{grid}\, t)}{f_s L} - \frac{2(V_{CAP})\sin^2(\omega_{grid}\, t)}{V_1 f_s L} \tag{10}$$

The inductor was dimensioned for a worst case scenario, the moment when there is the greatest ripple current in it. Hence, the maximum point was used, where the derivative is zero. Then (10) gives to (11).

$$\sin(\omega_{grid}\, t) = \frac{v_1}{4 V_{CAp}} \tag{11}$$

The equation (11) that determines the maximum ripple in the inductor NPC . Substituting (11) into (10) gives rise to (12), which is the expression that finds the value of the NPC inductor.

$$L = \frac{V_1}{8 f_s \Delta I_{Lmax}} \tag{12}$$

3) Dimensioning of NPC bus capacitors: The analysis was carried out on one of the capacitors of the inverter bus, but the calculations are validated for both. From Fig. 5, the instantaneous input power at the inverter can be written as (13).

$$P_1(t) = V_{CAp}\, I_{Lp} \sin^2(\omega_{grid}\, t) \tag{13}$$

Where: P_1 is the input power of the inverter NPC; I_{1p} peak input current in the NPC inverter.

The voltage V_{CA} has no angular displacement and is sinusoidal, by using trigonometric relations (14) is obtained.

$$P_{out}(t) = P_{outmed} - P_{outmed} \cos(2\omega_{rede}\, t) \tag{14}$$

From (14) it can be observed that the instantaneous output power of the inverter has two parts, one constant and one alternating power. By analysis the currents i_1, i_{S1} and i_{C1} it can be seen that i_{S1} has an average value equivalent to i1 added to the undulation of i_{C1}. Because of this characteristic, (15) can be obtained.

$$v_{c1} i_{c1} = P_{med} \cos(2\omega_{grid}\, t) \tag{15}$$

By considering the maximum ripple in the capacitor and Using the voltage equation in a Capacitor , (16) is obtained.

$$C_1 = \frac{P_{med}}{\omega_{grid}\, V_{C1} \Delta V_{C1max}} \tag{16}$$

Where: ΔV_{C1max} is the maximum ripple in the capacitor of the NPC

V. MODELING AND OBTAINING THE INVERTER TRANSFERFUNCTION

To obtain the current (internal transfer function) and voltage (external transfer function) loops of the NPC inverter, two different methods were used. Fig. 6 shows the block diagram of the loops that are of used for control.

A. Internal transfer function

In order to evaluate the internal transfer function it is enough to apply the linearization method by Jacobian in (6) and then to apply Laplace, gives rise to (17).

$$G_1(s) = \frac{I_L(s)}{D(s)} = \frac{V_1}{2L_s} \qquad (17)$$

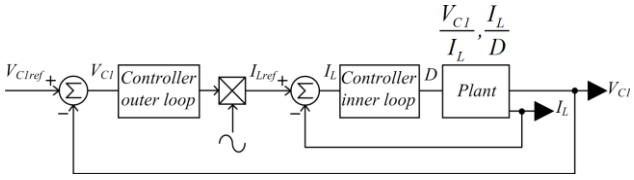

Fig. 5 Block diagram of control loops

B. External transfer function

To evaluate the external transfer function of the NPC, its modeling was considered as a rectifier and its energy flow was inverted, as shown in Fig. 7.

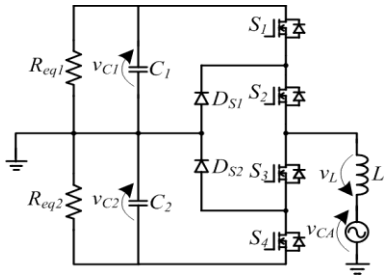

Fig. 6 NPC as rectifier

The NPC operation steps seen as a rectifier has four stages and it should be analyzed. It is necessary to analyze the first two steps, as done earlier. Thus, the equivalent circuits shown in Fig.7and Fig.8 can be obtained.

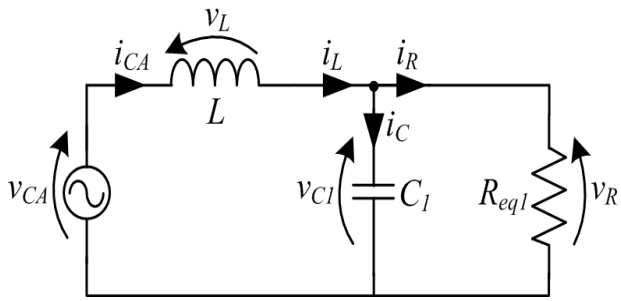

Fig.7 Equivalent circuit of the first step of the NPC as rectifier

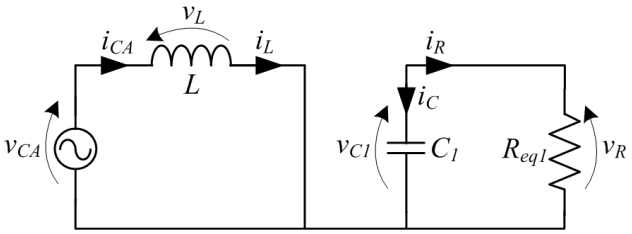

Fig. 8 Equivalent circuit of the second step of the NPC as rectifier

The mesh and nodal analysis are done on circuits of circuits of fig.8 and fig.9in order to evaluate differential equations referring to the inductors and capacitor of the circuit. By conducting a weighted average in these equations we have (18) and (19), which represent the non-linearized state equations of the inverter. Being (19) applicable to theotherNPCbuscapacitor.

$$\frac{di_L}{dt} = \frac{v_{CA}}{L} - \frac{v_1}{2L}D \tag{18}$$

$$\frac{dv_{C1}}{dt} = \frac{i_L}{C_1}D - \frac{v_{C1}}{R_{eq1}C_1} \tag{19}$$

The linearization of (18) and (19) was conducted around an operating point, using the Jacobian technique [17]. The linearized equations of (18) are in form of state space resulting in (20) and (21).

$$\begin{bmatrix} \frac{di_L}{dt} \\ \frac{dv_{C1}}{dt} \end{bmatrix} = \begin{bmatrix} 0 & -\frac{\overline{D}}{L} \\ \frac{\overline{D}}{C_1} & -\frac{1}{R_{eq1}} \end{bmatrix} \begin{bmatrix} I_L \\ V_{C1} \end{bmatrix} + \begin{bmatrix} -\frac{\overline{V}_{C1}}{L} \\ \frac{\overline{I}_L}{C_1} \end{bmatrix} [D] \tag{20}$$

$$y = [0 \quad 1] \begin{bmatrix} I_L \\ V_{C1} \end{bmatrix} \tag{21}$$

The bars on some variables are to explain that they are constant and considered in steady state. By using (20) and (21) it is possible to obtain the transfer function that relates the voltage across the capacitor C1 with the duty cycle following the methodology in [18]. This gives rise to (22).

$$G_2(s) = \frac{V_{C!}(s)}{D(s)} = \frac{\overline{V}_{C!}}{\overline{D}} \frac{1 - s\frac{L\bar{I}_L}{V_{C!}\overline{D}}}{1 + s\frac{L}{D^2 R_{eq1}} + S^2\frac{L_{C1}}{\overline{D^2}}} \tag{22}$$

To get the transfer function relating the current to the inductor with the duty cycle, it is needed to reverse the output of (21). Thus, it gives (23).

$$y = [0 \quad 1] \begin{bmatrix} I_L \\ V_{C1} \end{bmatrix} \tag{23}$$

Following the same method results in (22) through (23), (24) is obtained.

$$G_3(s) = \frac{I_l(s)}{D(s)} = \frac{-R_{eq1}LC_1\left(s\frac{\overline{V}_{C1}}{L} + \frac{\overline{V}_{C1}}{R_{eq1}LC_!} + \frac{\overline{DI}_L}{LC_1}\right)}{\overline{D^2}R_{eq1} + sL + s^2 R_{eq1}LC_1} \tag{24}$$

There is an important note that (24) represents the current injected into the grid with variations in the cyclic ratio from the point of view of the capacitance of the DC bus capacitors. In order to acquire the external transfer function, it is enough to divide (22)by (24), which gives rise (25).

$$G_4(s) = \frac{V_{c1}(s)}{I_l(s)} = \frac{\overline{V}_{C1}\overline{D} - sL\bar{I}_L}{sC_1\overline{V_{C1}} + \frac{\overline{V_{C1}}}{R_{eq1}} + \overline{DI_L}} \tag{25}$$

The (17) and (25) are the internal and external transfer functions used to obtain the circuit control loops.

VI.SIMULATION AND RESULT

The proposed ANFIS BASED Single-Phase Dual-Stage Isolated Multilevel Inverter Applied to Solar Energy Processing is simulated in mat lab. The simulation circuit mainly consist two stages. In the first stage consist of a DC-DC resonant converter and a transformer. In the second stage graetz circuits and a NPC inverter. The solar PV panel is connected to the DC-DC resonant converter. A capacitor is connected is placed in parallel in between the PV panel and converter in order to protect the converter from sudden changes in the load. In DC-DC resonant converter MOSFET having resistance of 0.1 ohms is used. The limbs of the converter A, B, C are connected to the capacitors C_{f1}, C_{f2}, C_{f3} and then to the transformer. The capacitors are mainly in a view that to protect the transformer from sudden changes in the load.

In the second stage one set secondaries of transformer is connected to the Graetz circuit and another set of secondaries are connected to another Graetz circuit. A NPC inverter is employed in the second stage after the Graetz circuit. Here the system is 3-wire system in order for grounding purpose the NPC is needed. Two capacitors C_1, C2 are placed in series in between the Graetz circuit and NPC inverter in way to protect the inverter from sudden changes in the load. The NPC inverter consist 4 switches S1, S2, S3, S4 connected in series. The Diodes D_{s1},D_{s2} are connected in between the switches S1 and S4. Those diodes D_{s1}, D_{s2} are freewheeling diodes. Then the terminals of entire circuit is connected to the load . As the load changes from time to time the load terminals are connected to the ANFIS controller as the controller manages the load by set of statements given by us.Fig.10 shows the simulink block Diagram. Fig.11 shows the ANFIS controller implemented. After implementation of simulink diagram shown in figure 12 ANFIS controller with an reference voltage(vref) as 260 volts the outputs noticed are voltage across the NPC bus(v1):500V,Solar panel voltage (Varray):400v,The Out Power as (Pout):2KW,The Load current (IL) as :20ohms.THD in the grid was reduced to 4.40 from 5.04.So there reduction of THD in the grid. The capacitive voltage drop is also reduced as compared to earlier as shown in the figure .12

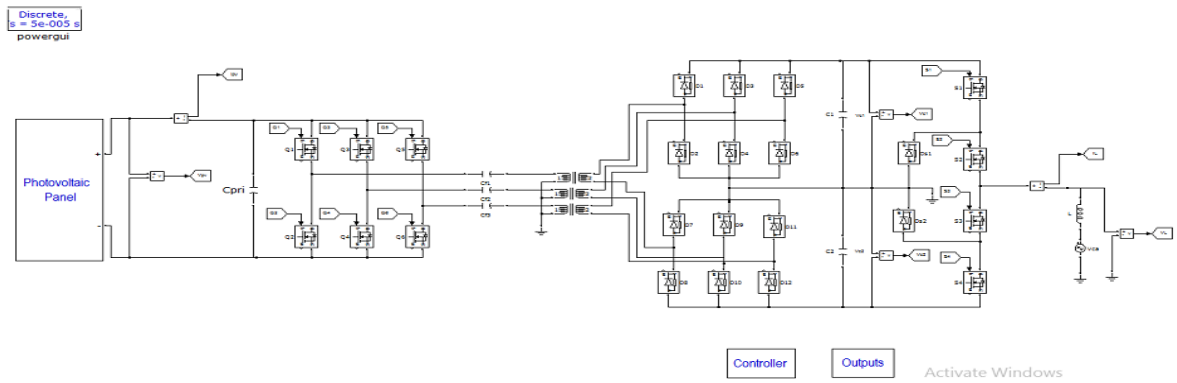

Fig. 9 shows the simulink diagram of proposed model

As the load is varying from time to time the load terminals are connected to the ANFIS controllerm in order to maintain the load . A set of statements are given to ANFIS in order to maintain the sudden changes in load and by using ANFIS controller need no to maintainn separate control for the load. The ANFIS controller connected to the load terminals in order to generate pulses is shown in figure.10

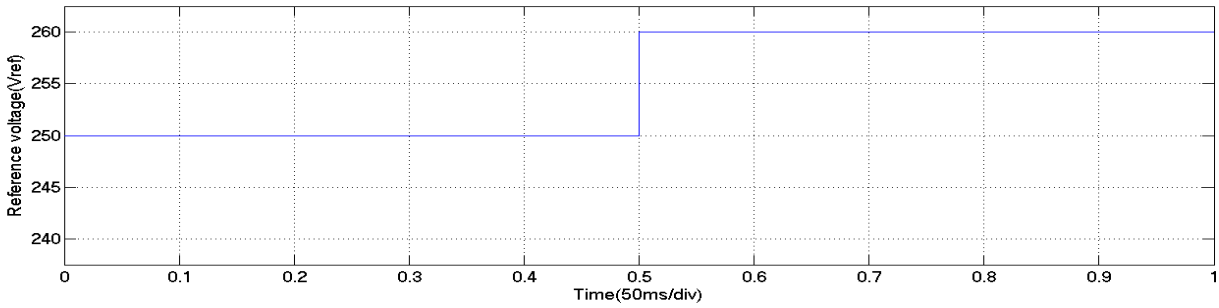

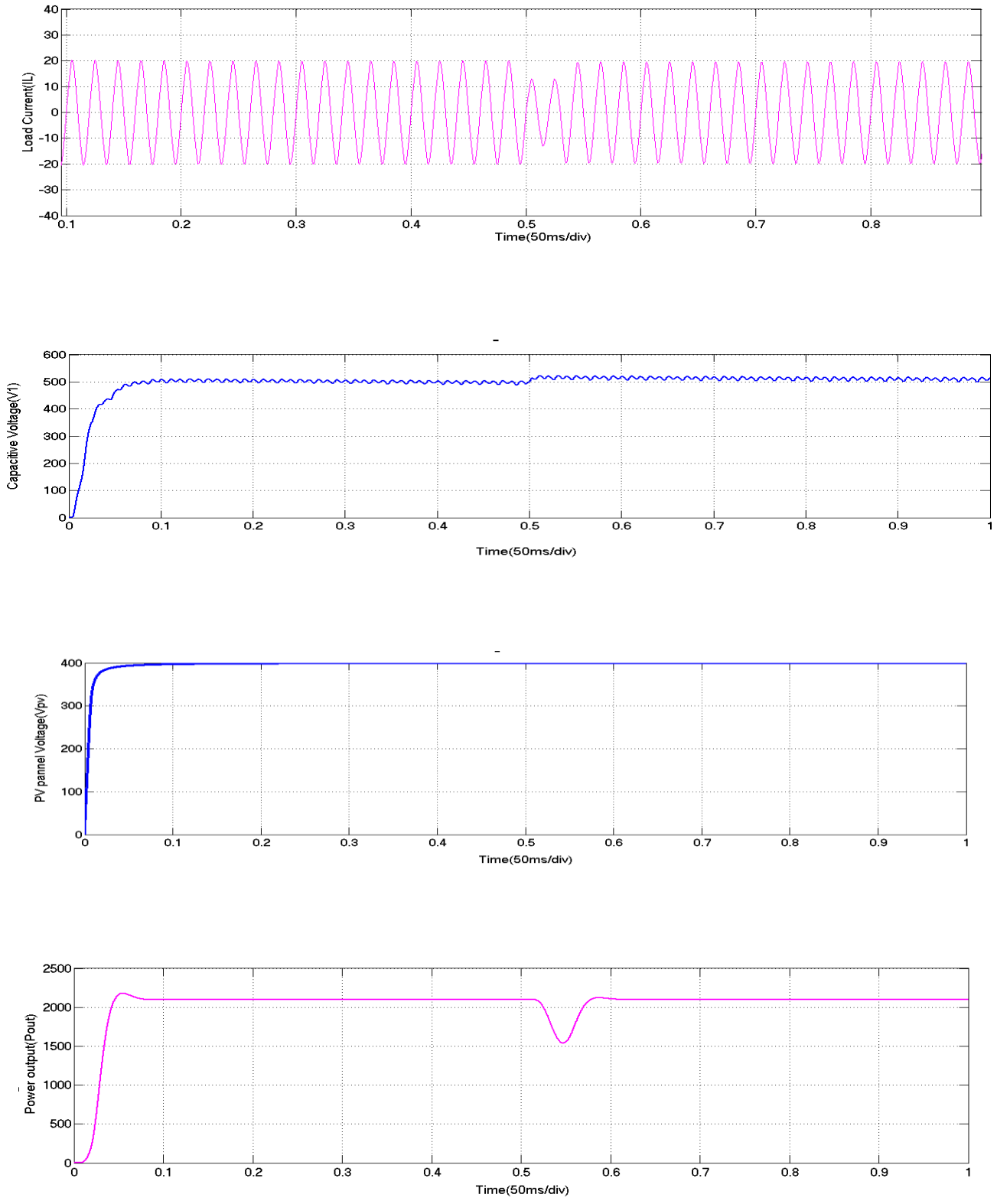

Fig.11: Simulation of the system with the ANFIS Controller. (a) Reference voltage Vref, (b) Load current IL, (c) load voltage VL, (d)Capacitive voltage V1, (e)Power output(Pout).

VII.CONCLUSION

In this paper a new configuration of a two-stage inverter was proposed. It is consist of a DC-DC converter with the purpose of obtaining at its output an equally divided voltage bus and a multilevel inverter responsible for injecting current into the grid. The modeling and control of the two stage inverter was implemented in order to inject electricity into the grid. With the simulation data, it is possible to verify the performance of the control over the structure, reinforcing that the methodology created presents a response that is consistent with that expected for this application. A proposal for future work is to build a prototype to verify its behavior in practice in order to validate the simulations results.

REFERENCES

[1] AgenciaNacional de EnergiaEletrica (Brazil), "Atlas de energiaeletrica do Brasil.," 2008.

[2] D. Watts and R. Ariztia, "The electricity crises of California, Brazil and Chile: lessons to the Chilean market," in *Power Engineering 2002 Large Engineering Systems Conference on, LESCOPE 02*, 2002, pp. 7–12.

[3] Frankfurt School, "Global Trends in Renewable Energy Investment 2015," 2015. [Online]. Available: http://fsunep-centre.org/publications/global-trends-renewable-energyinvestment- 2015. [Accessed: 20-Jan-2016].

[4] F. C. Mattos, V. S. Lacerda, R. L. Valle, A. A. Ferreira, P. G. Barbosa, and H. A. C. Braga, "Contribution To The Study Of A Single-Phase And Single Stage Photovoltaic System," *IEEE Lat. Am. Trans.*, vol. 13, no. 5, pp. 1265–1271, May 2015.

[5] K. C. A. de Souza, R. F. Coelho, and D. C. Martins, Proposta de um Sistema Fotovoltaico de DoisEstagiosConectado a RedeEletricaComercial," *Rev. EletronicaPotencia*, vol. 12, no. 2, pp. 129–136, 2007.

[6] M. Mao, Y. Zheng, L. Chang, and H. Xu, "A singlestage high gain current source inverter for grid-connected photovoltaic system," in *Power Electronics and ECCE Asia (ICPE-ECCE Asia), 2015 9th International Conference on*, 2015, pp. 1902–1907.

[7] Y. Kim, H. Cha, B.-M. Song, and K. Y. Lee, "Design and control of a grid-connected three-phase 3-level NPC inverter for Building Integrated Photovoltaic systems," in *2012 IEEE PES Innovative Smart Grid Technologies (ISGT)*, 2012, pp. 1–7

[8] T. Kerekes, R. Teodorescu, P. Rodriguez, G. Vazquez, and E. Aldabas, "A New High-Efficiency Single- Phase Transformerless PV Inverter Topology," *IEEE Trans. Ind. Electron.*, vol. 58, no. 1, pp. 184–191, Jan. 2011.

[9] N. Lekgamheng and Y. Kumsuwan, "Power analysis of single-phase grid-connected photovoltaic systems based on two-stage current source converters," in *Electrical Engineering/Electronics, Computer, Telecommunications and Information Technology (ECTI-CON), 2012 9th International Conference on*, 2012, pp. 1–4.

[10] A. Nabae, I. Takahashi, and H. Akagi, "A New Neutral-Point-Clamped PWM Inverter," *IEEE Trans. Ind. Appl.*, vol. IA-17, no. 5, pp. 518–523, Sep. 1981.

[11] B. Wu, *High-power converters and AC drives*. Hoboken, NJ: Wiley-Interscience [u.a.], 2006.

[12] M. M. Casaro and D. C. Martins, "Processamentoeletronico da energia solar fotovoltaicaemsistemasconectados a redeeletrica," *SbaControle Amp Autom. Soc. Bras. Autom.*, vol. 21, no. 2, pp. 159–172, Apr. 2010.

[13] J. Jacobs, A. Averberg, and R. De Doncker, "A novel three-phase DC/DC converter for high-power applications," in *Power Electronics Specialists Conference, 2004. PESC 04. 2004 IEEE 35th Annual*, 2004, vol. 3, pp. 1861–1867.

[14] R. Petrella, N. Buonocunto, A. Revelant, and P. Stocco, "Equalization of dc bus voltage in three-level NPC half-brige inverters for PV applications by even harmonics injection or fundamental phase modulation," in *2011 IEEE Energy Conversion Congress and Exposition*, 2011, pp. 3427– 3434.

[15] A. R. Prasad, P. D. Ziogas, and S. Manias, "Analysis and design of a three-phase offline DC-DC converter with high frequency isolation," in *, Conference Record of the 1988 IEEE Industry Applications Society Annual Meeting, 1988*, 1988, pp. 813–820 vol.1.

[16] H. Xiang, Y. Yan, and H. Jiang, "A two-stage PV grid-connected inverter with optimized anti-islanding protection method," in *2009 International Conference on Sustainable Power Generation and Supply*, 2009, pp. 1–4.

[17] C.-T. Chen, *Linear system theory and design*, 3. ed., 3. print. New York: Oxford Univ. Press, 1999.

[18] K. Ogata and B. Severo, *Engenharia de controlemoderno*. Rio de Janeiro: Prentice Hall do Brasil, 1998.